Image Quality Analysis for a Multiple Overlapping Field of View Serial Laser Imager

Nicholas Rasoletti[(1)], Fraser Dalgleish[(2)], Bing Ouyang[(2)], Anni Vuorenkoski[(2)] and Pierre-Philippe Beaujean[(1)]

(1) Department of Ocean and Mechanical Engineering
Center for Acoustics and Vibrations
Florida Atlantic University, Seatech
101 N. Beach Road, Dania Beach, FL 33004

(2) Harbor Branch Oceanographic Institute (HBOI) Ocean Visibility and Optics Laboratory
Florida Atlantic University
Ft. Pierce, FL 34946

The Combined Laser and Scan Sonar (CLASS) system is an extended range imaging system, incorporating both high-resolution laser images and high frequency sonar images. Both the laser and sonar images are collected simultaneously during testing to provide dual mode imagery of an underwater target, displaying both a 2D image of the target (laser image) and a 3D overlay of the target (sonar image). The laser component of the system is a Multiple Overlapping Field of view Serial Laser Imager (MOFSLI), capable of generating high-resolution sub-centimeter 2D images. MOFSLI generates the images by way of a diffraction-limited 532nm continuous wave (CW) laser beam being scanned over the target. Initial field tests resulted in high-quality images of the ocean floor. However, there was a clear need for further study and improvement. The first step is to carefully evaluate the quality of the images generated by MOFSLI. To do so, a calibration and performance evaluation of MOFSLI was executed in the specialized underwater electro-optics testing facility located in the Ocean Visibility and Optics laboratory at Harbor Branch Oceanographic Institute(HBOI), focusing on the effects of increased scattering levels.

I. INTRODUCTION

A. Scientific Background

The physical process of light propagation through water is governed by the radiative transfer equation [1][2]. This equation is based on radiative transfer theory, which is commonly broken up into two major categories: *inherent* optical properties, which are properties of the medium that are independent of the ambient light field, and *apparent* optical properties, which are dependent on the ambient light field. Inherent optical properties consist of absorption and scattering properties of the medium. When a photon interacts with a suspended particle within a volume of water, it can be either absorbed, in which case it is removed entirely from the medium, or it can be scattered, meaning its path is redirected in another direction. The fundamental inherent optical properties for these processes are the absorption coefficient, $a(\lambda)$, and the volume scattering function, $\beta(\psi,\lambda)$, respectively, where λ is the wavelength of the light within the medium and ψ is the scattering angle [3]. As the research described in this paper was conducted in a controlled testing environment, the apparent optical properties had minimal impact on the results, so they will not be elaborated on herein.

The MOFSLI system is a minimal moving parts version of a laser line scan (LLS) or synchronous scan imager, which utilizes multiple staring detectors that can be gain-controlled to maintain a flat angular response and high dynamic range throughout a wide range of optical turbidities. The two-axis transmit angles of the laser scanner are also software controllable, enabling fine-scale adjustments in the laser-receiver overlap functions in response to changes in stand-off distance and target orientation. These grayscale images display high contrast of objects on or near the ocean floor, allowing operators to identify surveyed objects. The main goal of this research is to characterize the changes in image performance of the adjacent sectors of the MOFSLI sensor due to increasing effects of absorption and scattering from suspended particles.

This is a DRAFT. As such it may not be cited in other works. The citable Proceedings of the Conference will be published in IEEE Xplore shortly after the conclusion of the conference.

In the longer term we are pursuing the development of automated imager control and correction algorithms that adaptively improve contrast of the collected images over a wide range of operating conditions.

B. Objectives and Contributions

Prior published field tests revealed high-quality imagery of the ocean floor, but left a clear need for further study [4]. Initial testing of the MOFSLI system was performed in clear coastal conditions, which did not fully evaluate the performance of this system. For the system to be viable for high resolution imaging tasks at extended ranges, e.g. to identify various corals and other indigenous reef inhabitants, it must be able to generate sub-centimeter image resolution in more turbid coastal conditions. Therefore, the immediate objectives of this research are to:

1) Evaluate the resolution, contrast and signal-to-noise ratio of the images collected throughout a controlled and well-characterized range of turbidities from clear water to turbid coastal conditions, which would correlate to a beam attenuation coefficient (*c*) which would vary between 0.1 [m^{-1}] to 1 [m^{-1}].
2) Develop a robust image processing algorithm to form high quality composite images and investigate gain control or image equalization techniques to improve signal to noise ratio, particularly in more turbid conditions. This second objective is not covered in this paper.

Rigorous calibration of this imaging device, was accomplished through optimizing both the laser and receiver angles for a certain distance, as well as determining the proper gain to be used based on monitoring of the received signal levels. Such approaches are critical if one wants to increase the overall effectiveness of the system. This type of imager has numerous uses that can aid scientific advancements, anything from studying underwater habitats to mine countermeasures to inspection, surveillance and reconnaissance missions [5][4].

II. METHODS AND MATERIALS

A. Theory

To improve the quality of the images generated by MOFSLI, a detailed calibration and performance evaluation of MOFSLI was executed in a specialized *electro-optics and LiDAR particle suspension test facility* located in the *Ocean Visibility and Optics Laboratory* at Harbor Branch Oceanographic Institute (HBOI). This environment allowed for carefully controlled testing conditions. During testing, the following characteristics of the system and environment were varied: The laser power output, the voltage gain of the PMTs, the distance between the laser and the target, and the turbidity of the water within the tank.

B. MOFSLI System Description

Controlling the MOFSLI system can be broken down into four major components (Figure 1). The central component is the computer, which is used to control the system, as well as store and process the collected data. The transmitter housing is serially connected to the host computer, and is powered by a battery located in a separate housing. The receiver housing is also connected to the computer, using two converter boxes, the Digi Edgeport converter box and a National Instruments data acquisition system (NI-DAQ). The receiver housing is connected directly into a 12V DC power supply.

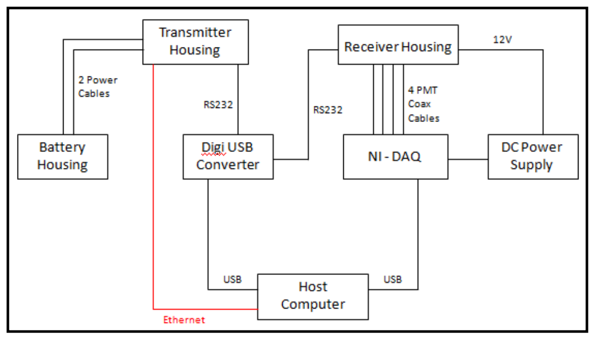

Figure 1: Diagram of MOFSLI control system

During the original field tests presented in [4], the transmitter and receiver housings were mounted onto the bracket shown in Figure 2. The separation between the transmitter and receiver housings was 1.13 [m]. The image below also depicts the sonar system, which would be used during field tests, but was not used during this calibration process.

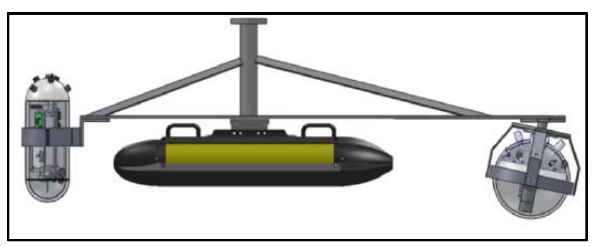

Figure 2: MOFSLI mounting bracket for at-sea test.

This mounting bracket was originally designed for boat use, while the calibration takes place in a test tank. To simulate both near-field and far-field conditions, testing took place at offsets of 4

[m] and 8 [m] within the test tank. A standing bracket was designed for the test tank (Figure 3).

Figure 3: Standing bracket for MOFSLI tank test.

a) Transmitter Housing

Housed inside the transmitter housing is a 1W 532 nm continuous wave green laser. Previous modifications were made to the system to better suit the MOFSLI prototype [4]. The laser beam was directed at the appropriate angle by way of a scanning galvanometer mirror. This mirror can make very fine adjustments (0.2365˚) to the along-track angle of the laser scan, adjustments that are controlled via a single-board real-time control system called EC1000. The computer communicates with the EC1000 via an Ethernet connection to send scanning commands.

b) Receiver Housing

The emitted laser beam light bounces off the target and reflects back toward the receiver unit. The MOFSLI receiver housing contains four collector assemblies (Figure 4), arranged in an overlapping linear array of telescopes. The prototype MOFSLI only has four detectors in the array, covering a total swath of some 30 degrees; it can be considered as a subset of a very wide angle system that is currently under development. The field-of-view of each telescope is fan-shaped due to the location of a slit aperture at the focal point of a F/0.8 lens, which is followed by the photocathode of the PMT. Each telescope therefore successively focuses the collected photons reflected from a successive target region onto a photocathode to form an image. These PMTs, model Hamamatsu R9880U-210, are extremely sensitive to a broad spectrum of light (ultraviolet, visible, and near-infrared), making them ideal for collecting reflected laser light [6]. However, to block out-of-band light with an extinction ratio of 10^{-5}, each 50mm diameter PMT assembly uses a 3nm full width at half maximum (FWHM) interference filter manufactured by Materion, which is centered at 532nm.

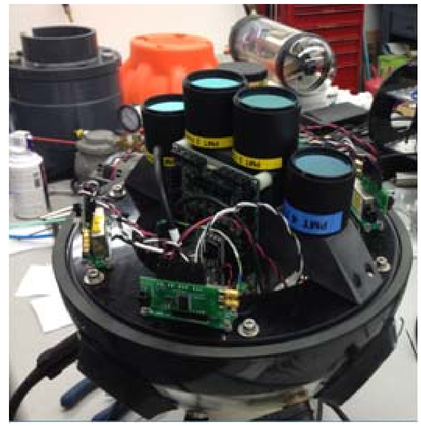

Figure 4: Open receiver housing showing the 4 collector assemblies (PMTs).

Throughout the paper, the four collector assemblies are referred to simply as PMTs, but they are actually made up of a band pass filter, slit aperture, lens, and the PMT itself. The band pass filter only allows certain wavelengths of light to pass though, thus filtering out light not originating from the green laser source. The slit aperture works to further reduce the amount of light reaching the PMT. By reducing the amount of light reaching the sensor, the slit apertures helps to cut down both forward scattered and back scattered laser light [4]. The collector assemblies were positioned in such a way that they would have overlapping fields of view, with of total cross track field of view of ±16˚. The horizontal swath, based upon this angle, was 2.29 [m] for the 4 [m] test, and 5.58 [m] for the 8 [m] test. The vertical beam width for the scanning of a single line measured approximately 1.5 [mm]. The vertical swathe range of the system is 30.745˚. This is the range of the system that will allow for optimal results, as later shown in Figure 10.

C. Testing Software

The transmitter unit is programmed to execute predefined scan jobs, typically following a zig-zag pattern. To do so, the host computer creates and loads a series of instructions to the EC1000. On the receiver side, a graphical user interface (GUI) which was developed in LabVIEW, allows for the remote control of the PMTs via gain adjustments. The GUI also displays near-real-time images of the data, while also allowing for the operator to set the number of scan lines. These data files are exported to MATLAB for further analysis. Figure 5 shows a screenshot of the LabVIEW GUI.

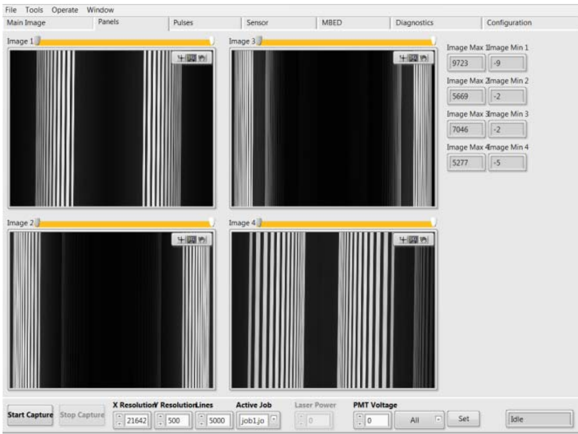

Figure 5: Example of experimental results using the LabVIEW interface.

III. EXPERIMENTATION

A. Test Setup

Figure 6 shows an overview of the calibration experiment. The MOFSLI system, lowered into the test tank via a modular crane located within the laboratory, sits on the bottom at one end of the tank, while the target is attached to the moving catwalk allowing for the distance between the MOFSLI and the target to be adjusted by moving the catwalk.

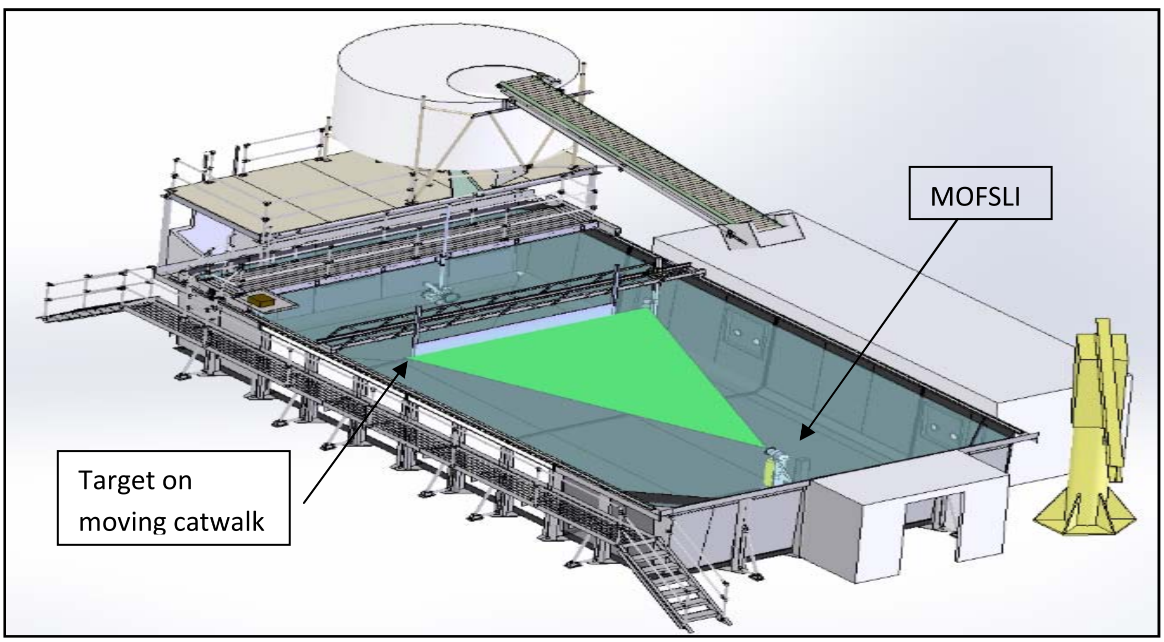

Figure 6: MOFSLI test setup.

Extensive testing of the MOFSLI system was accomplished by making adjustments to the following four parameters: the laser power output, the voltage gain of the PMTs, the distance between the laser and the target, and the turbidity of the water between the laser and the target. Testing was performed at laser powers of 101 [mW], 465 [mW], and 891 [mW]. PMT gains of 600 [V], 650 [V], 700 [V], and 750 [V] were tested, resulting in 14 bit dynamic range images (anywhere from 1000 to 32000 digital counts in clear water). These gains strictly came from the PMT (there was no amplifier used). To simulate both near-field and far-field conditions, testing took place at offsets of 4 [m] and 8 [m] within the test tank. At each of the offset distances, two scan jobs were chosen. Every scan jobs corresponded to a specific vertical height on the target. At 4 [m] offset, the vertical separation between scan jobs was 1.65 [cm]. At 8 [m] offset, the vertical separation between scan jobs was 3.3 [cm]. For every scan job, the laser was scanning horizontally from left-to-right and right-to-left at 195 lines per second. The cross track resolution of the images was 21642 pixels, while the along-track resolution was 5000 pixels.

B. Turbidity Levels in the Tank

Initial testing was representative of very clear water field conditions. After running the clear water testing, which established a baseline for the tank, the turbidity (which is to say, the attenuation coefficient c(λ)) of the water was adjusted by adding specific increments of ultrafine Arizona road dust. A total of nine turbidity levels (including clear water) were tested, ranging in attenuation coefficient values from 0.12 m^{-1} to 0.98 m^{-1}, correcting for scattering errors. A WET Labs AC-9 transmissometer monitored the spectral absorption and attenuation coefficients at all times during the experiment [7].

Water jets positioned around the tank were turned on during testing, keeping the current in the tank moving so as not to allow the suspended particles to settle on the bottom of the tank. The jets were at the top of the water, near the middle of the water column, and near the bottom of the tank, to ensure uniform flow. Since doing this could potentially lead to scattering errors due to larger particles entering the field of view, the measurements attained via the AC-9, with attenuation and absorption being adjusted for scattering error according to Zaneveld [8].

C. Targets

At each of the testing offset distances, two targets were used, a totally black target and a technical target. The black target was used for uniform reflectance, to accurately measure the decrease in received intensity as the turbidity levels of the water increased. Measuring 6.09 [m] by 56 [cm], the target was attached to a moving catwalk, allowing for the target to be moved to the different offset distances as needed. Mounted directly to the black target, the technical targets were made of a series of vertical bars, alternating between reflectance values of 3.4% and 26.6% with a band thickness ranging from 1 [mm] to 25 [mm]. This layout allowed for the determination of image contrast ratio and contrast signal-to-noise ratio, two metrics showing how the smaller bars gradually become unresolvable as the turbidity levels and associated scattering levels increased. The target reflectance levels were determined based on comparing the PMT voltage responses of the targets against targets of known reflectance known as spectralon medallions (Figure 7). A medallion of 50% reflectance was used and run through some of the same trials as the technical targets, and the results were compared, resulting in the reflectance values of the technical targets.

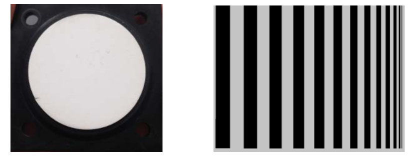

Figure 7: Spectralon medallion (left) and target for the four meter test.

The target for the four meter test measured 34.9 [cm] long x 27.6 [cm] wide. The target alternated black and white bars. Every other bar, the bar width decreased by 1 [mm]. The target for the eight meter test measured 97.1 [cm] long by 27.6 [cm] wide, to accommodate the increased swath size at 8 [m] offset. For this wider target, the bar widths needed to be configured in a different manner to maximize the size of the target within the field of view. The target was broken down in the following manner:

There were two bars each (1 dark and one light) for bar widths 25 [mm] through 15 [mm], and four bars each for bar widths 14 [mm] though 6 [mm]. There were six bars at the 5 [mm] width, eight bars at the 4 [mm] width, and ten bars at the 3 [mm] through 1 [mm] bars. The larger number of bars of identical width proved useful as the turbidity levels increased.

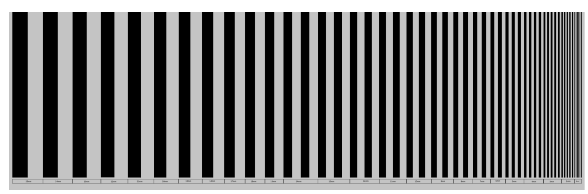

Figure 8: Target for the 8 meter test.

D. Controlling Ambient Light

The control of ambient light is crucial for all optical work. Stray light is equivalent to optical noise, which if present during testing could seriously alter the results. During this experiment, the major cause for concern was light scattering off the surface of the tank. Aside from light originating from other light sources within the lab, reflection off the water-air interface from scattered laser light within the tank has been shown to degrade the accuracy of the results. To deal with this, the HBOI laser lab uses multiple layers of small black plastic balls are all across the surface of the tank. These balls are buoyant, so they will stay on the surface. The balls act as a baffle for the surface of the entire tank, and hence remove most of the ambient light. Figure 9 shows how the balls on top of the water greatly diminish the reflectance of the laser light from the surface of the water.

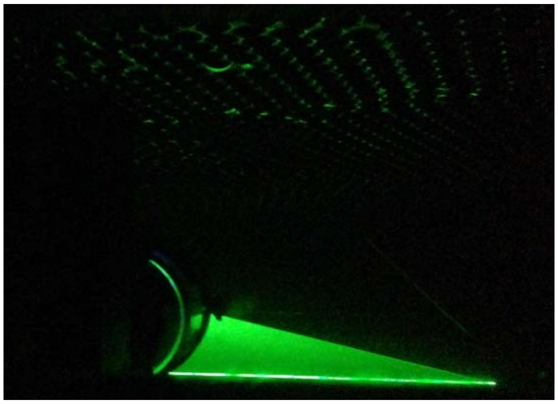

Figure 9: Plastic balls acting as buffer on surface.

IV. RESULTS

A. PMT field of view

The first objective of the testing was to determine the vertical field of view of each PMT. The purpose of this test was to determine which laser scan job (thus the vertical position of the laser beam) resulted in the highest signal recorded by each PMT (in terms of voltage across a 1KΩ load resistor within the digitizer). As a result, it was possible to identify the "optimal" vertical laser position for every PMT at a specific target offset distance (4 [m] or 8 [m]).

Prior to determining exactly which scan jobs would be optimal for this testing, a wide range of laser scan jobs encompassing the entire vertical swath-range of the system were run, and their vertical positions documented. Given their vertical position and offset distances, line equations could be developed for all possible laser scan job offsets within the swath range. With this done, determining the optimal scan job for the two offset distances would help to develop a line for the optimal receiver line of sight (slope). A series of trials were run, in which the only system parameter to change was the laser scan job, and the voltage response for each PMT was recorded. From these results, two jobs were chosen, one that best matched the peak values of the PMTs, the other further away, which allowed for a comparison to show how using an inaccurate scan job can affect the results. This test was run at both offset distances, revealing the four scan jobs that would be used for testing.

With this information, all the laser scan jobs (Tx) and the receiver line of sight (Rx) could be plotted (Figure 10). It is important to remember that the system is really looking sideways in the tank, while in a field application it would actually be looking down, as shown in Figure 10. This information allows the choosing of the proper scan job (as listed in the legend of Figure 10) without further testing at any depth up to 13.7 [m]. Note that the jobs listed encompass the entire swath range, which covers the laser swath angle of 30.745˚. Note that this was the vertical swath angle during this testing, but the system will be rotated for field tests.

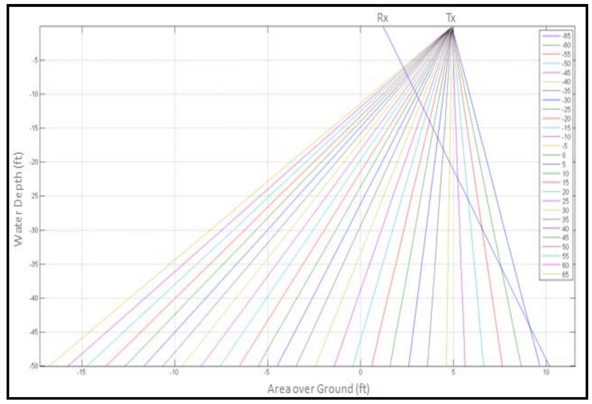

Figure 10: Laser rays for individual scan jobs (Tx) and optimal direction (Rx) for laser beam measurement at every PMT.

After determining the vertical field of view, the next step was to determine the horizontal field of view for each PMT. To do this, the technical targets were mounted edge-to-edge on the background target, starting on the edge of the laser scan job. Images were taken, and these images showed not only the extent over the targets that the PMTs FOV extended, but also showed where the sweet spot was located, as evidenced by stronger signal return. These positions were marked for all PMTs at both offset distances and later used for formal testing. Figure 11 shows a diagram depicting the general setup of the test.

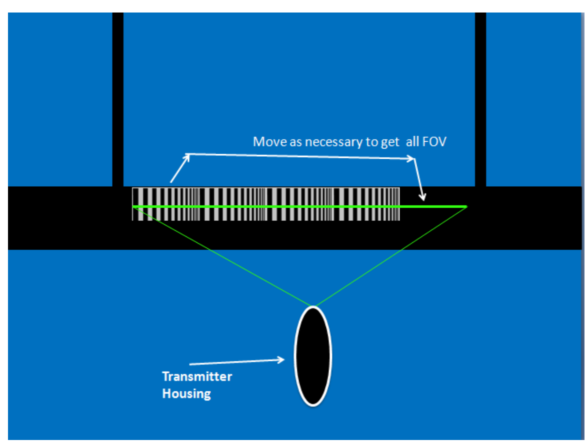

Figure 11: Determining the Horizontal PMT field of view.

B. Testing Results

Figures 12 and 13 illustrate how the conditions and results changed during testing. In these figures, the laser reached the target with two different turbidity levels, for a target offset distance of 4 [m].

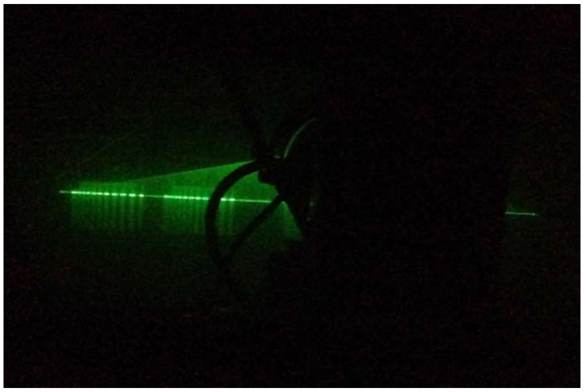

Figure 12: Laser illuminating the target located at 4 [m], with c(λ)= 0.141597.

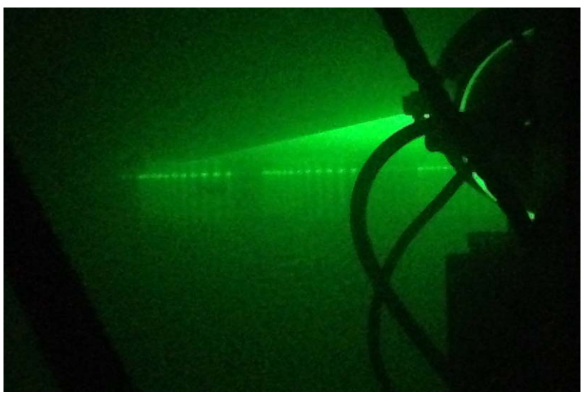

Figure 13: Laser illuminating the target located at 4 [m], with c(λ)= 0.492029.

The above images were shot though a viewing window into the tank from behind the MOFSLI system. Note that no ambient light came from this viewing window at any time during testing.

For processing to begin, the data were exported from LabVIEW and brought into MATLAB as binary files, in 16-bit gray scale format. The data were time-stamped, separated by channels (PMTs), and formatted in 2-D arrays (one per PMT). Every row of an array corresponds to a horizontal laser scan. Every column corresponds to the same point on the target (there is no vertical scanning).

Figures 14 to 16 show the image obtained when the target is located at 8 [m] for four different turbidity levels (c(λ)=0.14065, c(λ)=0.349659, c(λ)= 0.521891 and c(λ)= 0.628707) out of six turbidity levels, from clear water (c(λ)=0.14065) up to moderately turbid waters (c(λ)=0.736759). At c(λ)=0.736759, there was no discernible image of the target. There were nine attenuation levels tested for the 4 [m] offset distance, from clear water to c(λ)=0.979514.

Figure 14 indicates that the target elements remain distinguishable all the way down to 5 [mm] bar thickness in clear water. As the turbidity increases (Figure 15, with c(λ)=0.349659), bars remain visible down to 7 [mm] thickness. When c(λ)=0.521891 (Figure 16), bars remain visible down to 12 [mm] thickness.

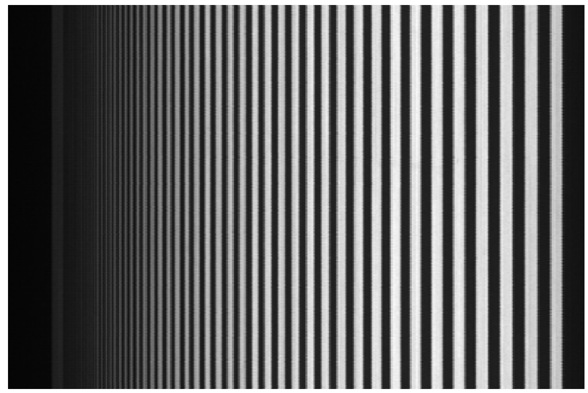

Figure 14: Image obtained when the target is located at 8 [m], c(λ)=0.14065.

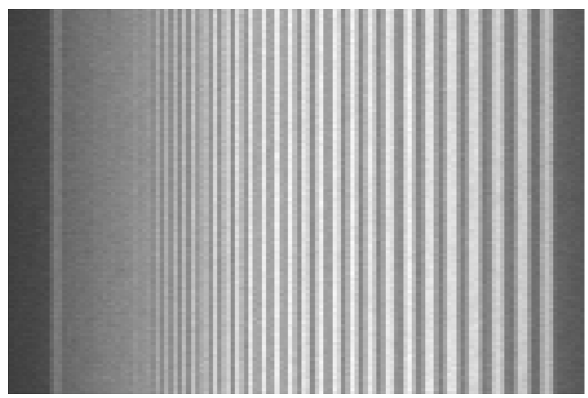

Figure 15: Image obtained when the target is located at 8 [m], c(λ)=0.349659.

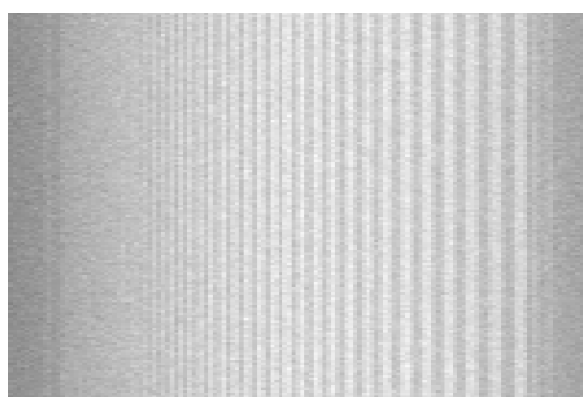

Figure 16: Image obtained when the target is located at 8 [m], c(λ)=0.521891.

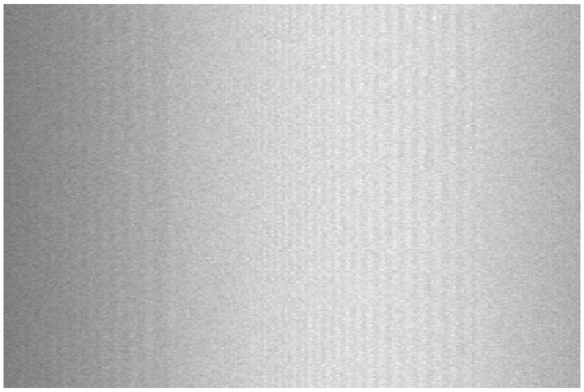

Figure 17: Image obtained when the target is located at 8 [m], c(λ)=0.628707.

C. Image Quality Analysis

The image quality evaluation process involved measuring the contrast and contrast signal-to-noise ratio (CSNR) of the captured target, as described by Dalgleish et al [9],

$$\text{Contrast Ratio} = \frac{\overline{I_{white}} - \overline{I_{black}}}{\overline{I_{white}} + \overline{I_{black}}}, \qquad (1)$$

$$\text{CSNR} = \frac{\overline{I_{white}} + \overline{I_{black}}}{\sqrt{Var[I_{white}] + Var[I_{black}]}}. \qquad (2)$$

Here $\overline{I_{white}}$ and $\overline{I_{black}}$ are the average intensities of the white and black portions of the target, respectively, while $Var[I_{white}]$ and $Var[I_{black}]$ are the intensity variances of the white and black portions. As previously noted, the reflectance level of the black bars was 3.4%, while the white bars had a reflectance level of 26.6%.

The following procedure was used to calculate the Contrast Ratio and the CSNR. For a given distance and PMT, the MATLAB program would display the image. The operator used a graphic tool to mark the center of the widest white band, and the center of the nearest black band. Following this, the program would select the four pixels closest to the center of the white band for 600 rows of the image, creating an array I_{white} of 2400 high intensity values. The program repeats the same process in the black band for an array I_{black} of 2400 low intensity values.

Figures 18 and 19 depict the contrast ratio and CSNR when the target is located at 8 [m] as they relate to the number of beam attenuation lengths (dimensionless parameter defined as the one way distance to target multiplied by $c(\lambda)$). The number of beam attenuation length varied from 1 to 5. The laser power was 891 [mW] and four PMT gains were used.

Figure 20 shows the voltage response of PMT 3 for each of the gains as it relates to the number of beam attenuation lengths, again with a laser power of 891 [mW].

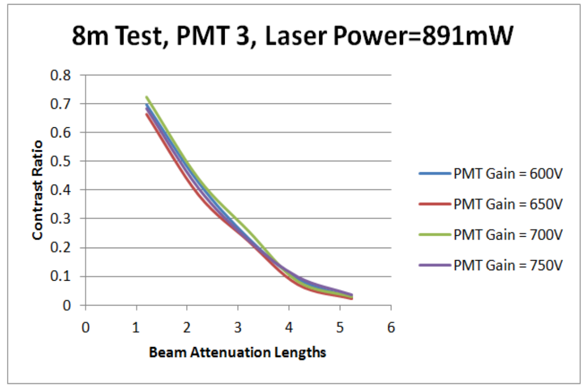

Figure 18: Contrast Ratio, target at 8 [m].

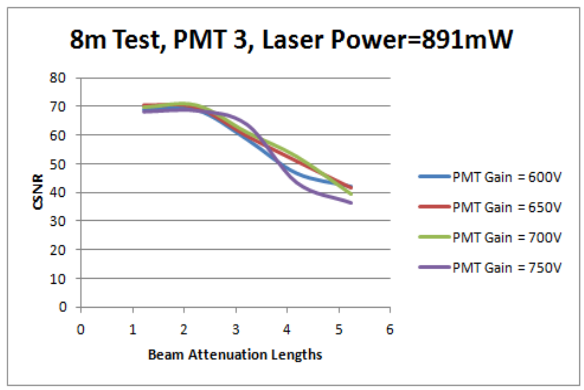

Figure 19: Contrast Signal-to-Noise Ratio, target at 8 [m].

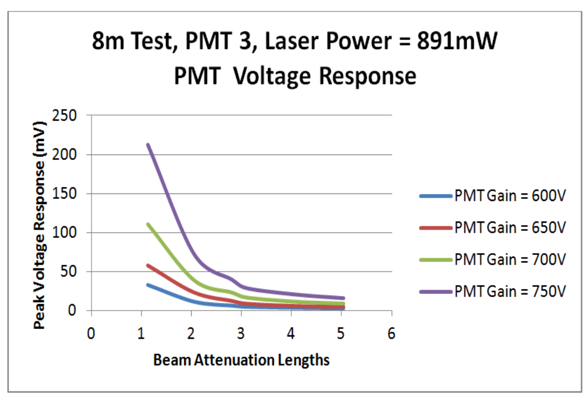

Figure 20: PMT Voltage Response as attenuation levels increase.

Figure 18 shows that the Contrast Ratio decreases linearly up to approximately two attenuation lengths. Beyond this, the Contrast Ratio continues decreasing in an increasingly non-linear manner up to five attenuation lengths, i.e. the five attenuation length case corresponds to the image shown in figure 17. This contrast limit is due to increased levels of both backscatter and attenuation in the water, both of which continue to rise as the water becomes more turbid, and eventually completely obscures any useful image data. Both the contrast ratio and CSNR plots appear to exhibit similar characteristics of previously accepted research, offering some validity to the results [9].

V. CONCLUSIONS AND FUTURE WORK

The main objective of the research presented in this paper was to evaluate the resolution, contrast ratio and contrast signal-to-noise ratio of the images collected throughout a controlled and well-characterized range of turbidities, in an effort to assess the effectiveness of the MOFSLI system in providing scientifically useful imagery at coral reef sites where the biological objects of interest range in size from several mm to several cm. Through observing the contrast and CSNR, this research revealed both the limits of the system, as well as how the image quality changed as its environment changed.

The MOFSLI system was demonstrated to exceed the performance range of cameras and lights, which typically become contrast limited in turbid waters prior to three attenuation lengths. However, over the stand-off distance (8 meters) and turbidities tested, the MOFSLI was ultimately contrast limited by the collection of non-image bearing photons (i.e. backscattering) at approximately 5 beam attenuation lengths. In order to eliminate this backscattered light, previous research has demonstrated that using a pulsed-gated serial laser system can allow for the generation of useful imagery beyond seven attenuation lengths. In the absence of backscattering, the loss of contrast and resolution at these extended ranges is believed to be due to the combined effects of attenuation and forward scattering, which causes the detrimental blurring or glow that obscures the image detail.

ACKNOWLEDGEMENTS

The authors would like to thank all the staff at Harbor Branch that assisted in the completion of this work, particularly Ben Metzger and Brian Ramos. We would also like to thank FAU and the Link Foundation for helping to fund this research.

REFERENCES

[1] C.F. Bohren & D.R. Huffman, Absorption and Scattering of Light by Small Particles, John Wiley & Sons, 1983.

[2] J. Downing, "Effects of Light Absorption and Scattering in Water Samples on OBS Measurements," Campbell Scientifici, Inc., 2008.

[3] C. Mobley, "Inherent Optical Properties - Ocean Optics Web Book," 16 February 2010. http://www.oceanopticsbook.info/view/overview_of_optical_oceanography/inherent_optical_properties.

[4] S. Parton, F.R. Dalgliesh, P.-P. Beaujean, B. Ouyang, F.M. Camini, "Acquisition and Registration of Bathymetric Acoustic Data and MOFSLI (Multiple Overlapping Field of View Serial Laser Imager)," in *OCEANS*, Bergen, 2013.

[5] M.P. Strand, "Quantitative evaluation of environmental noise in underwater electro-optic imaging systems," in *Ocean Optics XIV, Kailua-Kona, Hawaii. November 10-13, 1998*

[6] Hamamatsu Photonics K.K., "Photomultiplier Tubes - Basics and Applications - 3rd edition (3a)," Hamamatsu Photonics K.K., August 2007.

[7] J. Bower, U.C. Davis, "Spectrometer," http://chemwiki.ucdavis.edu/Analytical_Chemistry/Instrumental_Analysis/Spectrometer#References.

[8] J.R.V. Zaneveld, J.C. Kitchen, and C. Moore, "The scattering error correction of reflecting-tube absorption meters," *Ocean Optics XII, Proc. SPIE,* 2258, pp. 44-55, 1994.

[9] F.R. Dalgleish, F.M. Caimi, W.B. Britton, & C.F. Andren, "Improved LLS imaging performance in scattering-dominant waters," in *SPIE, Vol. 7317*, April 29, 2009.